

**Sodium Chloride interaction with solvated and crystalline cellulose :
sodium ion affects the tetramer and fibril in aqueous solution**

Giovanni Bellesia¹ and S. Gnanakaran²

¹⁾*Theoretical Biology and Biophysics Group, Center for Nonlinear Studies,
Los Alamos National Laboratory, Los Alamos, NM 87545,
USA^{a)}*

²⁾*Theoretical Biology and Biophysics Group, Los Alamos National Laboratory,
Los Alamos, NM 87545, USA*

(Dated: 30 October 2018)

Inorganic salts are a natural component of biomass which have a significant effect on the product yields from a variety of biomass conversion processes. Understanding their effect on biomass at the microscopic level can help discover their mechanistic role. We present a study of the effect of aqueous sodium chloride (NaCl) on the largest component of biomass, cellulose, focused on the thermodynamic and structural effect of a sodium ion on the cellulose tetramer, and fibril. Replica exchange molecular dynamics simulations of a cellulose tetramer reveal a number of preferred cellulose-Na contacts and bridging positions. Large scale MD simulations on a model cellulose fibril find that Na^+ perturbs the hydroxymethyl rotational state population and consequently disrupts the ‘native’ hydrogen bonding network.

Keywords: Biomass, Sodium Chloride, Molecular Dynamics, Conformations

^{a)}Electronic mail: giovanni.bellesia@gmail.com

I. INTRODUCTION

Inorganic salts are an integral part of any biomass material. Indeed, plant biomass naturally contains alkali and alkaline earth metals, including potassium, sodium, phosphorus, calcium, and magnesium.¹⁻³ While the total mineral content is less than 1 %, the effect, either adverse or favorable, on biomass degradation and product distribution is significant. Removal of these cations would add cost⁴ to biofuel production, which is already more costly than conventional petroleum-based fuels. Thus, it is preferable to understand how the inorganic material interacts with the biomass to better steer conversion toward more valuable products. In particular, a detailed understanding of the interactions between inorganic salts and biomass is of central importance for devising efficient biomass degradation protocols for bioenergy production.

In fast pyrolysis, the presence of inorganic salts has been shown to increase the yield of lower-value low-molecular weight species and adversely affects the formation of levoglucosan (the main pyrolysis product of pure cellulose).⁵ Conversely, in steam gasification of biomass-derived charcoal, Li, Na and K chlorides have been used as catalysts to increase gas yield and to reduce the operational temperature.⁶ The beneficial effect of inorganic salts has also been outlined in recent studies showing that the presence of NaCl increases the yield of levulinic acid in acid-catalyzed depolymerization of cellulose in water.^{7,8} Those studies are especially relevant as they combine low-price NaCl with relatively mild reaction conditions and low temperatures ($T = 373 - 473$ K). In those acid catalysis experiments the NaCl concentration varies in the range of 5 – 50% wt. The peak in the sugars' yield has been obtained with NaCl concentrations in the range of 20 – 30% wt. It is speculated that NaCl contributes to the destabilization of the highly-structured hydrogen bond network in cellulose, thereby increasing the efficiency of the cellulose hydrolysis process.

In our study we employ classical computational methods to study the atomistic details of the interactions of NaCl oligomeric and crystalline fibrillar cellulose. Oligomeric and crystalline fibrillar cellulose were studied via replica exchange molecular dynamics and via single temperature molecular dynamics (MD) simulations respectively.

Our results show that there are multiple positions for Na^+ to associate with hydroxyl groups of a pyranose ring within thermal energy ($k_B T$) at temperatures relevant to biomass conversion. Thus, it is expected that these ions could affect many different reactions and

thus have wide-ranging effects on decomposition of biomass.

II. COMPUTATIONAL METHODS

We performed replica exchange Langevin dynamics (LD) and single temperature NPT-LD simulations to analyze the equilibrium dynamics of a cellulose tetramer and of a model fibril of crystalline cellulose in NaCl aqueous solution, respectively. Replica Exchange LD simulations^{9,10} were carried out in a simulation box of dimensions $L_x = 38.8$ Å $L_y = 43.1$ Å and $L_z = 34.4$ Å containing 1839 water molecules and 5 NaCl pairs. The cellulose-NaCl ratio in the cellulose tetramer system corresponds to a 40 wt% concentration, which is within the range of the experimental wt% concentrations used in salt-assisted acidcatalysis experiments of cellulose decomposition.^{7,8} Forty-eight replicas were used corresponding to 48 temperatures in the interval $[298 - 550]$ K. The total simulation time per replica was 100 ns with *replica swaps* performed every 40 ps and a *swap acceptance ratio* varying between 0.1 and 0.3. The last 50 ns were considered for data analysis. The cellulose tetramer was capped with reducing and non-reducing ends.^{11,12} The tetramer and the ion pairs were spatially constrained within a sphere of radius $r_s = 15$ Å centered in the water box center.¹³ In more detail, spherical harmonic boundary conditions were enforced on the tetramer and the ion pairs by means of a single potential function,

$$E_s = \begin{cases} k_s(|\mathbf{r}_i - \mathbf{r}_c| - r_s)^2 & \text{if } |\mathbf{r}_i - \mathbf{r}_c| > r_s, \\ 0 & \text{otherwise} \end{cases} \quad (1)$$

where $k_s = 10$ kcal/mol, \mathbf{r}_i is the current position of atom i and \mathbf{r}_c is the center of the sphere. The potential E_s was used to increase the NaCl concentration (≈ 0.6 M) without increasing the size of the system and, therefore, the computational cost of the simulations. Additional Replica Exchange LD simulations were carried out for a cellulose tetramer in aqueous solution without NaCl under the same simulation conditions used in the NaCl simulations. For these calculations, the total simulation time per replica was 40 ns and the last 20 ns were considered for data analysis. Two single temperature NPT-LD simulations on a crystalline I_β cellulose fibril composed of 30 octameric glucan chains were performed at $T = 298$ K and $T = 400$ K. For the initial fibril conformation we considered an equilibrated structure from previous LD simulations.¹⁴ Each octameric cellulose chain was covalently connected to its periodic image along its main axis in order to mimic an infinitely long

cellulose fibril.¹⁴ The fibril was solvated in a rectangular box containing 6660 water molecules and 15 NaCl pairs. The cellulose-NaCl ratio in the cellulose fibril system corresponds to 2 wt%, which is within the concentration range present in real biomass feedstock (0.5 – 5%) and relevant to fast pyrolysis experiments.⁵ The 2 wt% concentration used in our simulations is close to the lowest concentration used in acid catalysis experiments (5% wt).^{7,8} The use of this relatively low NaCl concentration is justified by the fact that for higher concentrations (both in terms of weight percent and molarity), ions tend to form small unphysical clusters that strongly limit the NaCl reactivity and negatively affect the statistical sampling of the NaCl-cellulose interactions. This is a well known problem that arises when classical force fields are used.^{15,16}

The solvated cellulose fibril underwent first a local optimization, followed by a short (0.5 ns) NPT–MD simulation, where the temperature was gradually increased from 100 K to 298 K. This initial optimization-thermalization simulation was followed by two separate 100 ns long NPT–MD simulations at $T = 298$ K and $T = 400$ K, respectively. The pressure P was 1.01325 bar. The first 10 ns of the 100 ns run were considered as the initial equilibration time and the remaining 90 ns as the production time. During the 100 ns simulation runs we applied a cylindrical boundary potential (oriented along the cellulose fibril main axis) analogous to the one shown in Equation 1 using a radius $r_{cyl} = 35$ Å and an infinite length. We found that the magnitude of both the spherical and the cylindrical potential is negligible when compared to the total potential energy of our systems ($< 0.01\%$ of the total potential energy). Hence, we do not expect the presence of the boundary potentials to affect our results and conclusions. In addition, we used the same protocol to run a 50 ns simulation on a fibril in pure water at $T = 400$ K. In all simulations, the time step was fixed at 2.0 fs. The covalent bonds involving hydrogen atoms were constrained by means of the SHAKE algorithm.¹⁷ We used the NAMD software package¹⁸ with the GLYCAMO6¹⁹ force field and the TIP3P explicit water model.²⁰ The reliability of the GLYCAM force field for solvated and crystalline cellulose systems has been assessed in a number of recent publications.^{12,14,21,22} A Langevin thermostat and Nose–Hoover Langevin barostat with a stochastic component were used to control the temperature and the pressure, respectively.^{23,24} The damping coefficient for the Langevin integrator was set to 1.0 ps^{-1} , while for the Nose–Hoover Langevin barostat we applied an oscillation period of 200 fs and a damping period of 100 fs. The cutoff for the non-bonded interactions in the coordinate space was fixed at 10.0 Å. All the simula-

tions were performed under periodic boundary conditions, and the long-range electrostatic interactions were calculated by using the Ewald summation method with the particle mesh Ewald algorithm.²⁵ The particle mesh Ewald accuracy was fixed at 10^{-6} , the order of the interpolation functions on the grid was set to 4 and the grid spacing was ≈ 1.0 Å.

III. RESULTS AND DISCUSSION

A. Cellotetraose Conformations

Conformations of a cellulose tetramer have been analyzed considering a set of relevant dihedral degrees of freedom¹²: the hydroxymethyl rotational state^{12,14} and the three puckering angles defining the conformation of the glucose ring ($C2C3C4C5$, $C4C5O5C1$, $O5C1C2C3$). In Fig. 1(A) we plot the percentage for the three hydroxymethyl rotational states (tg , gt and gg) as a function of temperature. At 298 K, the rotational population is mostly dominated by the gg state with the gt state contributing as well. The statistical weight of the tg state (dominant in native crystalline cellulose) is quite small at room temperature. Not surprisingly, the statistical weight of tg increases with temperature as the thermal energy “flattens” the energy barriers between the three hydroxymethyl states. In Fig. S1(A,B,C) in the supplementary information we show the residuals between tg , gt and gg data, respectively, calculated as the difference between the percentages collected in NaCl aqueous solution (Fig. 1(A)) and the analogous data collected from the simulations of the cellulose tetramer in pure water. The normalized sums of the residuals are 0.27%, 1.20% and -1.47% , for tg , gt and gg , respectively. These data show that when NaCl is present, the statistical weight of the gg state diminishes mostly at the expense of the gt state that becomes moderately more favorable than in pure water.

In Fig. 1(B) we plot the percentage of distorted, non- 4C_1 conformations (black triangles) defined by negative values of at least one of the dihedrals $C2C3C4C5$, $C4C5O5C1$ and $O5C1C2C3$.¹² We also show the partial percentages for each of the three angles defining the ring conformation. The percentage of distorted, non-chair-like conformations appears to increase linearly with temperature. Comparison with simulations in pure water (Figure S1(D)) shows that the statistical weight of the non- 4C_1 conformations is negligible when NaCl is present (normalized residual = 1.15%).

B. Cellotetraose- Na^+ Interaction

To analyze the interaction of solvated cellulose with NaCl, and in particular with Na^+ , we first considered a set of radial distribution functions (RDFs) related to ion-cellulose heavy atom interactions. The limited number of ions in our system together with the lack of radial symmetry make the use of RDFs problematic, especially when it comes to normalization at large distances. Nevertheless, we make preliminary use of ion-cellulose RDFs to obtain information about the location of the first minimum which defines the cutoff distance for the ion-cellulose interactions (Fig. S2). A systematic analysis of the RDFs reveals that the most relevant ion-cellulose interactions involve Na^+ and the hydroxyl oxygen atoms. The sharp peaks near 2.5 Å indicate that Na^+ forms a well-defined coordination with hydroxyl groups. The peak is stronger in the O3- Na^+ case indicating that the coordination is stronger in this case. With increasing temperature, the peaks lose intensity and become slightly broader.

The first minimum in those critical RDFs is typically well-defined and located at a distance $r_c = 3.2$ Å. That distance represents an accurate cutoff measure for the first coordination cell and for defining “contacts” between Na^+ and oxygen atoms in cellulose. In Table I, we report the relative probabilities for the “contacts” between Na^+ ions and the relevant oxygen atoms O2, O3 and O6 (hydroxymethyl oxygen) in cellulose at $T = 298$, $T = 402$ and $T = 502$ K. Oxygens that belong to the non-reducing end of the cellulose tetramer are included in the calculations. Our results show that O3 is slightly more prone to form contacts with Na^+ than O6 and O2. The full temperature dependence for the relative probabilities of the O2- Na^+ , O3- Na^+ and O6- Na^+ contacts is shown in Fig. 2. The rotational flexibility of the hydroxymethyl group allows the relative probability for the O6- Na^+ contacts to increase with temperature and to become the largest at temperatures > 410 K. In the bottom part of Table I we show the results for the relative three-body contacts (joint probabilities) involving Na^+ , Ox and Oy ($x, y = 2, 3, 6$, $x \neq y$) at $T = 298$, $T = 402$ and $T = 502$ K. Full temperature dependence data show that the Na^+ coordination involving O2 and O3 atoms has, by far, the highest statistical weight across the temperature interval considered in our simulations.

In terms of intramolecular cellulose hydrogen bonding in both the NaCl and pure water simulations of the solvated tetramer, we observe a dominant O3 – O5 bond and marginal contributions from O6 – O3, O3 – O6, O6 – O2 and O2 – O6 hydrogen bonds. The percentage

contribution of the $O3 - O5$ hydrogen bond decreases linearly from $\sim 80 - 90\%$ to $\sim 57\%$ with temperature increasing from 298 K to 400 K. Conversely, the same temperature increase is associated with an increase in the percentage contribution of $O6 - O3$, $O3 - O6$, $O6 - O2$ and $O2 - O6$ hydrogen bonds together from $7 - 9\%$ to $23 - 25\%$ (data not shown).

C. Cellulose I_β Fibril

The comparison between the hydroxymethyl population in a model cellulose fibril in NaCl aqueous solution (at 298 and 400 K) and an identical fibril in pure water¹⁴ (at 298 and 400 K) is reported in Table II. The results show that the presence of NaCl perturbs the hydroxymethyl rotational state occupancy favoring the *gt* and *gg* conformations over *tg* in both the fibril crystalline core and its surface at both temperatures. At 400 K, the *gg* rotational state becomes the dominant one both on the fibril surface and in its crystalline core. Despite the change in the hydroxymethyl rotational state occupancy, due to the presence of NaCl, the fibril maintains I_β symmetry in its crystalline core at both 298 and 400 K (data not shown). We did not observe any non-chair-like conformation in our simulations of the cellulose fibrils (neither at 298 nor at 400 K).

D. Cellulose I_β Fibril- Na^+ Interaction

In III we report the results for the relevant two and three-body relative contact probabilities involving Na^+ and the cellulose oxygens Ox ($x = 2, 3, 6$) in a model cellulose fibril. The cellulose- Na^+ contacts analyzed in our study apply to the cellulose chains on the fibril surface and exposed directly to the solvent. We did not observe any substantial penetration of the Na^+ ions within the cellulose fibril. Single contacts are highly favored over bridging positions, and among those single contacts, *O6* has the highest probability of contact to Na^+ at both $T = 298$ and $T = 400$ K. The contacts between the cellulose oxygens *O2*, *O3*, *O6* and Na^+ account for over 70% of the total contacts between cellulose heavy atoms and $\text{Na}^+ \text{Cl}^-$ pairs. Specifically, the ratio between Cl^- and Na^+ contacts with the cellulose heavy atoms is 0.29 at 298 K and 0.27 at 400 K. *O2* shows the highest probability of contact to Cl^- at 298 K and 400 K. We did not observe any simultaneous contact between Cl^- and cellulose oxygen pairs (bridging positions).

The internal hydrogen bond for the cellulose fibril in the presence of NaCl shows some differences when compared with the results from simulations in pure water.¹⁴ When the hydroxymethyl group deviates from the *tg* conformation (typical of native crystalline cellulose) we expect the weakening (or the disappearance) of the native intramolecular hydrogen bonds involving the hydroxymethyl oxygen *O6* and the appearance of new hydrogen bonds connecting neighboring layers within the crystal.^{26,27} Indeed, a comparison with previous simulations in pure water¹⁴ shows that the presence of NaCl leads to a lower number of intramolecular hydrogen bonds (Fig. S3 and S4, top row) with the number decreasing with increasing temperature from 298 to 400 K, and a higher number of intersheet hydrogen bonds (Fig. S3 and S4, bottom row) with the number increasing with increasing temperature from 298 to 400 K. The intermolecular/intrasheet hydrogen bond network (Fig. S3 and S4, center row) does not seem to be perturbed by the presence of NaCl at 298 K. Conversely, at 400 K the presence of NaCl results in a lower number of intermolecular/intrasheet hydrogen bonds.

In Table IV we show the relative contributions to the cellulose-water hydrogen bond network at 298 K of oxygens *O2*, *O3*, *O6* for a model cellulose fibril with NaCl (Fib-NaCl) and without NaCl (Fib).¹⁴ Our data reveal that the presence of NaCl (even at relatively low concentrations - see Methods Section) results in a decrease of the relative contribution of the hydroxymethyl oxygen *O6* possibly due to its high relative affinity to Na^+ . Typically, the water coordination to *O3* is the lowest due to presence of persistent *O3* – *O5* intrachain hydrogen bond. Interestingly, a slight increase is seen in *O3* hydrogen bonding to water in the presence of NaCl. The cellulose-water hydrogen bonding maintains these same general trends also at 400 K in the crystalline cellulose simulations. Interestingly, for the solvated tetramer neither the presence of NaCl nor a change in temperature (in the interval 298 – 550 K) alters the relative contributions of the oxygens *O2*, *O3* and *O6* to the cellulose–water hydrogen bond network.

IV. CONCLUSION

Inorganic salts, in general and NaCl in particular, are known to adversely affect biomass fast pyrolysis and to increase the efficiency of catalytic cellulose degradation in the aqueous environment. The purpose of this computational study was to resolve the atomistic details of the interactions of oligomeric and fibrillar forms of solvated cellulose with Na^+ .

Our classical MD simulations show that the dominant interaction is the one between the Na^+ and the hydroxyl oxygen atoms in cellulose.

In more detail, we observe that, in cellulose, the two backbone oxygens *O2*, *O3* and the sidechain oxygen *O6* account for most of the interactions with Na^+ , with the hydroxymethyl oxygen *O6* dominating at high temperatures (> 410 K) in solvated cellulose and at both 298 K and 400 K in crystalline cellulose. In solvated cellulose, we also noticed a high affinity for Na^+ to be in a “bridging” position between the *O2* and *O3* backbone oxygens.

Our simulations also show only minor structural changes in the pyranose ring due to the presence of NaCl. The chair conformation was the dominant ring structure for both oligomeric and crystalline cellulose in the classical MD simulations. In crystalline cellulose, the presence of NaCl perturbs the rotational state population of the hydroxymethyl group. As a consequence of the perturbation of the hydroxymethyl rotational state population, the hydrogen bonding network in crystalline cellulose is also perturbed by the presence of NaCl. In particular we observed the disappearance of a number of intramolecular hydrogen bonds and a consequential emergence of intersheet hydrogen bonds as seen previously in the high temperature MD simulations of native cellulose and cellulose III_I^{14,28}. The enhanced understanding of the interactions of sodium chloride with cellulose gained from this computational study will provide valuable information for the design of cost-effective thermochemical degradation protocols for cellulosic biomass.

V. ACKNOWLEDGEMENTS

This work was supported by CNLS and LANL Institutional Computing.

REFERENCES

- ¹D. Mohan, C. U. Pittman, Jr., and P. H. Steele, “Pyrolysis of Wood/Biomass for Bio-oil: A Critical Review,” *Energy Fuels*, **20**, 848 (2006), ISSN 0887-0624.
- ²P. R. Patwardhan, J. A. Satrio, R. C. Brown, and B. H. Shanks, “Product Distribution from Fast Pyrolysis of Glucose-Based Carbohydrates,” *J. Anal. Appl. Pyrolysis*, **86**, 323 (2009), ISSN 01652370.

- ³P. R. Patwardhan, R. C. Brown, and B. H. Shanks, "Product Distribution from the Fast Pyrolysis of Hemicellulose." *ChemSusChem*, **4**, 636 (2011), ISSN 1864-564X.
- ⁴D. S. Scott, L. Paterson, J. Piskorz, and D. Radlein, "Pretreatment of Poplar Wood for Fast Pyrolysis: Rate of Cation Removal," *J. Anal. Appl. Pyrolysis*, **57**, 169 (2001).
- ⁵P. R. Patwardhan, J. A. Satrio, R. C. Brown, and B. H. Shanks, "Influence of inorganic salts on the primary pyrolysis products of cellulose," *Bioresour. Technol.*, **101**, 4646 (2010).
- ⁶J. M. Encinar, J. F. González, J. J. Rodríguez, and M. J. Ramiro, "Catalysed and uncatalysed steam gasification of eucalyptus char: influence of variables and kinetic study," *Fuel*, **80**, 2025 (2001).
- ⁷T. vom Stein, P. Grande, F. Sibilla, U. Commandeur, R. Fischer, W. Leitner, and P. Dominguez de Maria, "Salt-assisted organic-acid-catalyzed depolymerization of cellulose," *Green Chem.*, **12**, 1844 (2010).
- ⁸J. Potvin, E. Sorlien, J. Hegner, B. DeBoef, and B. L. Lucht, "Effect of nacl on the conversion of cellulose to glucose and levulinic acid," *Tetrahedron Lett.*, **52**, 5891 (2011).
- ⁹R. Swensen and J. Wang, "Replica monte carlo simulation of spin glasses," *Phys. Rev. Lett.*, **57**, 2607 (1986).
- ¹⁰Y. Sugita and Y. Okamoto, "Replica exchange molecular dynamics method for protein folding," *Chem. Phys. Lett.*, **314**, 141 (1999).
- ¹¹<http://glycam.ccruc.uga.edu/AMBER/index.html>.
- ¹²T. Shen, P. Langan, A. D. French, G. P. Johnson, and S. Gnanakaran, "Conformational flexibility of soluble cellulose oligomers: chain length and temperature dependence." *J. Am. Chem. Soc.*, **131**, 14786 (2009).
- ¹³G. Bellesia and J.-E. Shea, "What determines the structure and stability of kffe monomers, dimers and protofibrils," *Biophys. J.*, **96**, 875 (2009).
- ¹⁴S. P. Chundawat, G. Bellesia, N. Uppugundla, L. da Costa Sousa, D. Gao, A. Cheh, U. P. Agarwal, C. M. Bianchetti, G. N. J. Phillips, P. Langan, V. Balan, S. Gnanakaran, and B. E. Dale, "Restructuring crystalline cellulose hydrogen bond network enhances its depolymerization rate," *J. Am. Chem. Soc.*, **133**, 11163 (2011).
- ¹⁵J. Wang, P. Cieplak, and P. Kollman, "How well does a restrained electrostatic potential (resp) model perform in calculating energies of organic and biological molecules ?" *J. Comput. Chem.*, **21**, 1049 (2000).

- ¹⁶A. A. Chen and R. V. Pappu, "Parameters of monovalent ions in the amber99 forcefield: assessment of inaccuracies and proposed improvements," *J. Phys. Chem. B*, **111**, 11884 (2007).
- ¹⁷J. Ryckaert, G. Ciccotti, and H. Berendsen, "Numerical integration of the cartesian equations of motion of a system with constraints: Molecular dynamics of n-alkanes," *J. Comput. Phys.*, **23**, 327 (1977).
- ¹⁸J. Phillips, R. Braun, W. Wang, J. Gumbart, E. Tajkhorshid, E. Villa, C. Chipot, R. Skeel, L. Kale, and K. Schulten, "Scalable molecular dynamics with namd," *J. Comput. Chem.*, **26**, 1781 (2005).
- ¹⁹K. Kirschner, A. Yongye, S. Tschampel, J. González-Outeiriño, C. Daniels, L. Foley, and R. Woods, "Glycam06: A generalizable biomolecular force field. carbohydrates," *J. Comput. Chem.*, **29**, 622 (2008), ISSN 1096-987X.
- ²⁰W. L. Jorgensen, J. Chandrasekhar, M. J. D, R. W. Impey, and K. M. L, "Comparison of simple potential functions for simulating liquid water," *J. Chem. Phys.*, **79**, 926 (1983).
- ²¹G. Bellesia, S. P. S. Chundawat, P. Langan, B. E. Dale, and S. Gnanakaran, "Probing the early events associated with liquid ammonia pretreatment of native crystalline cellulose," *Journal of Physical Chemistry B*, **115**, 9782 (2011).
- ²²J. Matthews, G. Beckham, M. Bergensträhle-Wohlert, J. Brady, M. Himmel, and M. Crowley, "Comparison of cellulose i β simulations with three carbohydrate force fields," *Journal of Chemical Theory and Computation*, **8**, 735 (2012).
- ²³S. Feller, Y. Zhang, R. Pastor, and B. Brooks, "Constant pressure molecular dynamics simulation: The langevin piston method," *J. Chem. Phys.*, **103**, 4613 (1995).
- ²⁴G. J. Martyna, D. J. Tobias, and K. M. L, "Constant pressure molecular dynamics algorithms," *J. Chem. Phys.*, **101**, 4177 (1994).
- ²⁵T. Darden, D. York, and L. Pedersen, "Particle mesh ewald: An nlog(n) method for ewald sums in large systems," *J. Chem. Phys.*, **98**, 10089 (1993).
- ²⁶Y. Nishiyama, P. Langan, and H. Chanzy, "Crystal structure and hydrogen-bonding system in cellulose i β from synchrotron x-ray and neutron fiber diffraction." *J. Am. Chem. Soc.*, **124**, 9074 (2002).
- ²⁷M. Wada, H. Chanzy, Y. Nishiyama, and P. Langan, "Cellulose iii(i) crystal structure and hydrogen bonding by synchrotron x-ray and neutron fiber diffraction," *Macromolecules*, **37**, 8548 (2004).

- ²⁸J. F. Matthews, M. Bergenstråhle, G. T. Beckham, M. E. Himmel, M. R. Nimlos, J. W. Brady, and M. F. Crowley, “High-temperature behavior of cellulose i,” *The Journal of Physical Chemistry B*, **115**, 2155 (2011), <http://pubs.acs.org/doi/pdf/10.1021/jp1106839>.

TABLE I. Cellulose tetramer in NaCl aqueous solution. Two and three-body relative contact probabilities between Na^+ and cellulose oxygens Ox where $x = 2, 3, 6$. For example, the two-body relative contact probability between Na^+ ions and $O6$ oxygens is calculated as $P(\text{Na} - O6) = \text{Na} - O6 - \text{contacts} / (\text{Na} - O2 - \text{contacts} + \text{Na} - O3 - \text{contacts} + \text{Na} - O6 - \text{contacts})$ while the three-body contact probability between Na^+ ions, $O3$ and $O6$ is calculated as $P(\text{Na} - O3 - O6) = \text{Na} - O3 - O6 - \text{contacts} / (\text{Na} - O3 - \text{contacts} + \text{Na} - O6 - \text{contacts})$.

| T(K) | O2 | O3 | O6 |
|------|-------------|-------------|-------------|
| 298 | 0.32 | 0.37 | 0.30 |
| 402 | 0.34 | 0.33 | 0.32 |
| 502 | 0.32 | 0.32 | 0.35 |
| T(K) | O2-O3 | O2-O6 | O3-O6 |
| 298 | 0.22 | 0.02 | 0.10 |
| 402 | 0.17 | 0.02 | 0.07 |
| 502 | 0.15 | 0.02 | 0.07 |

TABLE II. Rotational state occupancy for the hydroxymethyl group in the fibril crystalline core and on the surface cellulose chains in cellulose I_β fibrils in pure water at 298 K (Fib-298)¹⁴, in NaCl aqueous solution at 298 K (Fib-298-NaCl) and at 400 K (Fib-400-NaCl).

| Fib-298 ¹⁴ | <i>tg</i> | <i>gt</i> | <i>gg</i> |
|-----------------------|-----------|-----------|-----------|
| crystalline core | 92.8% | 4.6 | 2.6 |
| surface chains | 25.8% | 28.1 | 46.1 |
| Fib-298-NaCl | <i>tg</i> | <i>gt</i> | <i>gg</i> |
| crystalline core | 59.9% | 25.2 | 14.9 |
| surface chains | 15.7% | 37.1 | 47.2 |
| Fib-400 | <i>tg</i> | <i>gt</i> | <i>gg</i> |
| crystalline core | 54.5 | 14.8 | 30.7 |
| surface chains | 18.1 | 28.4 | 53.5 |
| Fib-400-NaCl | <i>tg</i> | <i>gt</i> | <i>gg</i> |
| crystalline core | 9.3% | 43.7 | 47.0 |
| surface chains | 11.4% | 35.1 | 53.5 |

TABLE III. Cellulose I_β fibril in NaCl aqueous solution. Two and three-body relative contact probabilities between Na^+ and cellulose oxygens Ox where $x = 2, 3, 6$. For example, the two-body relative contact probability between Na^+ ions and $O6$ oxygens is calculated as $P(\text{Na} - O6) = \text{Na} - O6 - \text{contacts} / (\text{Na} - O2 - \text{contacts} + \text{Na} - O3 - \text{contacts} + \text{Na} - O6 - \text{contacts})$ while the three-body contact probability between Na^+ ions, $O3$ and $O6$ is calculated as $P(\text{Na} - O3 - O6) = \text{Na} - O3 - O6 - \text{contacts} / (\text{Na} - O3 - \text{contacts} + \text{Na} - O6 - \text{contacts})$.

| T(K) | O2 | O3 | O6 |
|------|-------|-------|-------------|
| 298 | 0.24 | 0.33 | 0.41 |
| 400 | 0.18 | 0.35 | 0.46 |
| T(K) | O2-O3 | O2-O6 | O3-O6 |
| 298 | 0.05 | 0.06 | 0.06 |
| 400 | 0.08 | 0.06 | 0.08 |

TABLE IV. Relative contribution to the cellulose–water hydrogen bond network at 298 K of oxygens O2, O3, and O6. Comparison between fibril with NaCl (Fib-NaCl) and fibril without NaCl (Fib).¹⁴

| System | O2 | O3 | O6 |
|----------|------|-------------|-------------|
| Fib-NaCl | 0.29 | 0.32 | 0.27 |
| Fib | 0.31 | 0.24 | 0.35 |

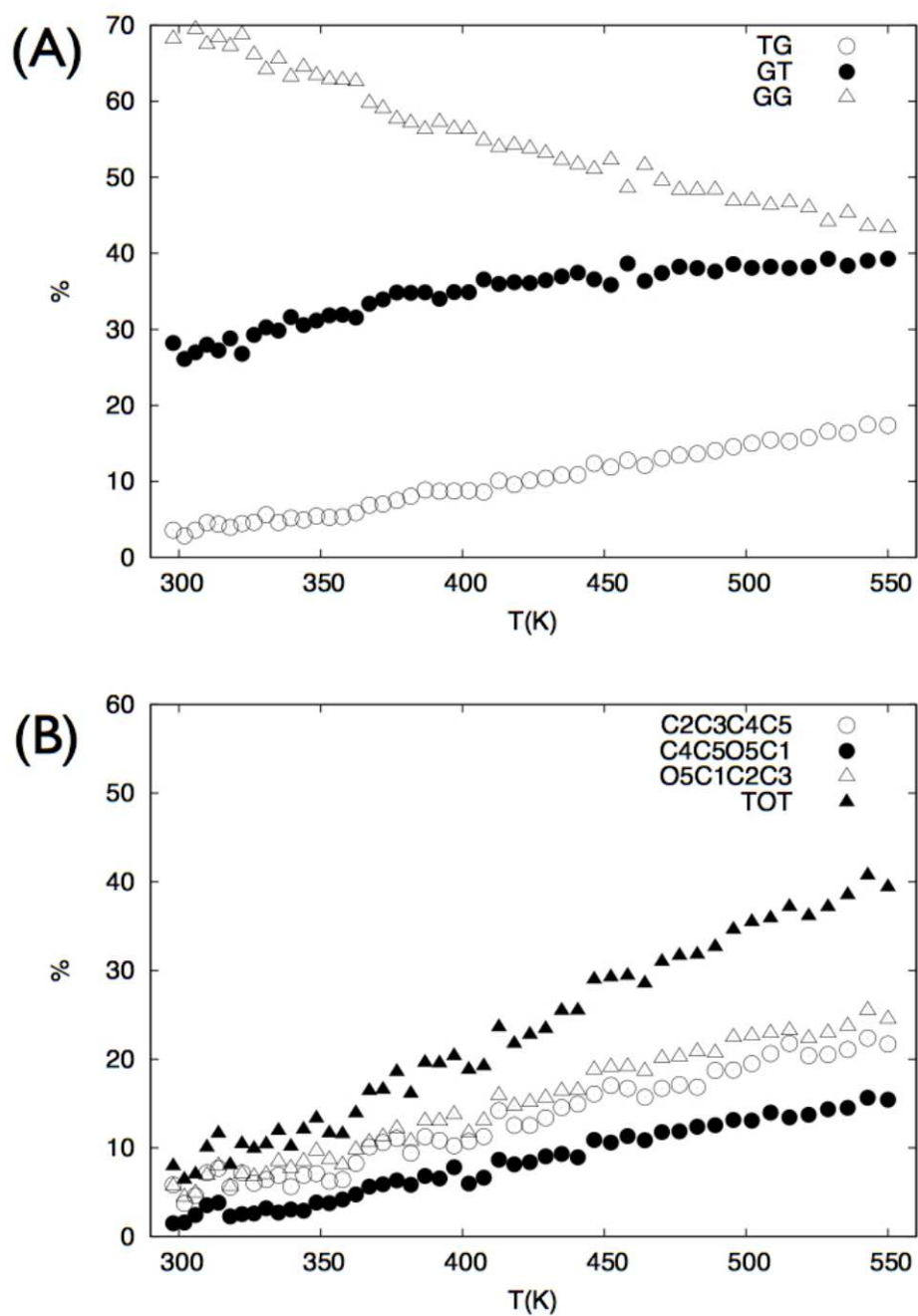


FIG. 1. (A) Percentage of the rotational state population for the hydroxymethyl group as a function of temperature. (B) Percentage for the non chair-like conformation of the glucose rings as a function of temperature. Results are shown for each of the three dihedral angles defining the ring conformation as well as for the total percentage of non-chair-like conformations (black triangles).

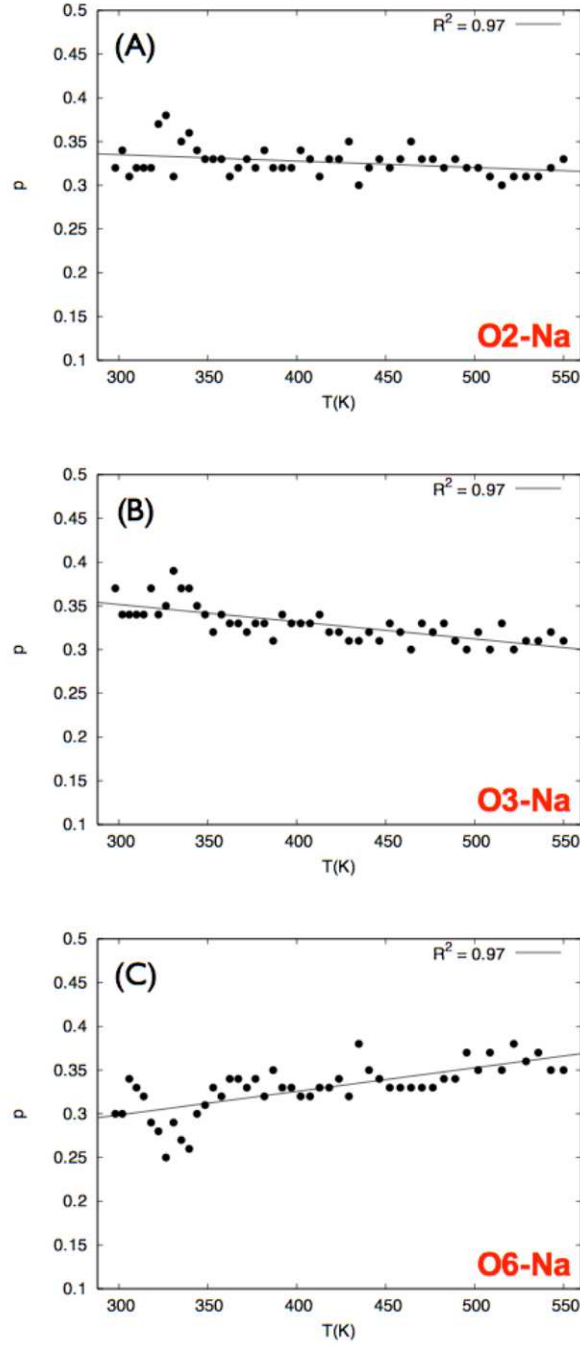


FIG. 2. Cellulose tetramer in NaCl aqueous solution. Full temperature dependence of the relative probabilities of O2-Na⁺, O3-Na⁺, O6-Na⁺ contacts are shown in panels (A), (B) and (C), respectively. O6 increases its contact probability to Na⁺ at higher temperatures. At ~ 410 K, O6 contact probability to Na⁺ becomes the largest.

Supporting information for:

Sodium Chloride interaction with solvated and

crystalline cellulose :

sodium ion affects the tetramer and fibril in aqueous

solution

Giovanni Bellesia[†] and S. Gnanakaran^{*,‡}

Theoretical Biology and Biophysics Group, Center for Nonlinear Studies, Los Alamos National Laboratory, Los Alamos, NM 87545, USA, and Theoretical Biology and Biophysics Group, Los Alamos National Laboratory, Los Alamos, NM 87545, USA

E-mail: gnana@lanl.gov

*To whom correspondence should be addressed

[†]Theoretical Biology and Biophysics Group, Center for Nonlinear Studies, Los Alamos National Laboratory, Los Alamos, NM 87545, USA

[‡]Theoretical Biology and Biophysics Group, Los Alamos National Laboratory, Los Alamos, NM 87545, USA

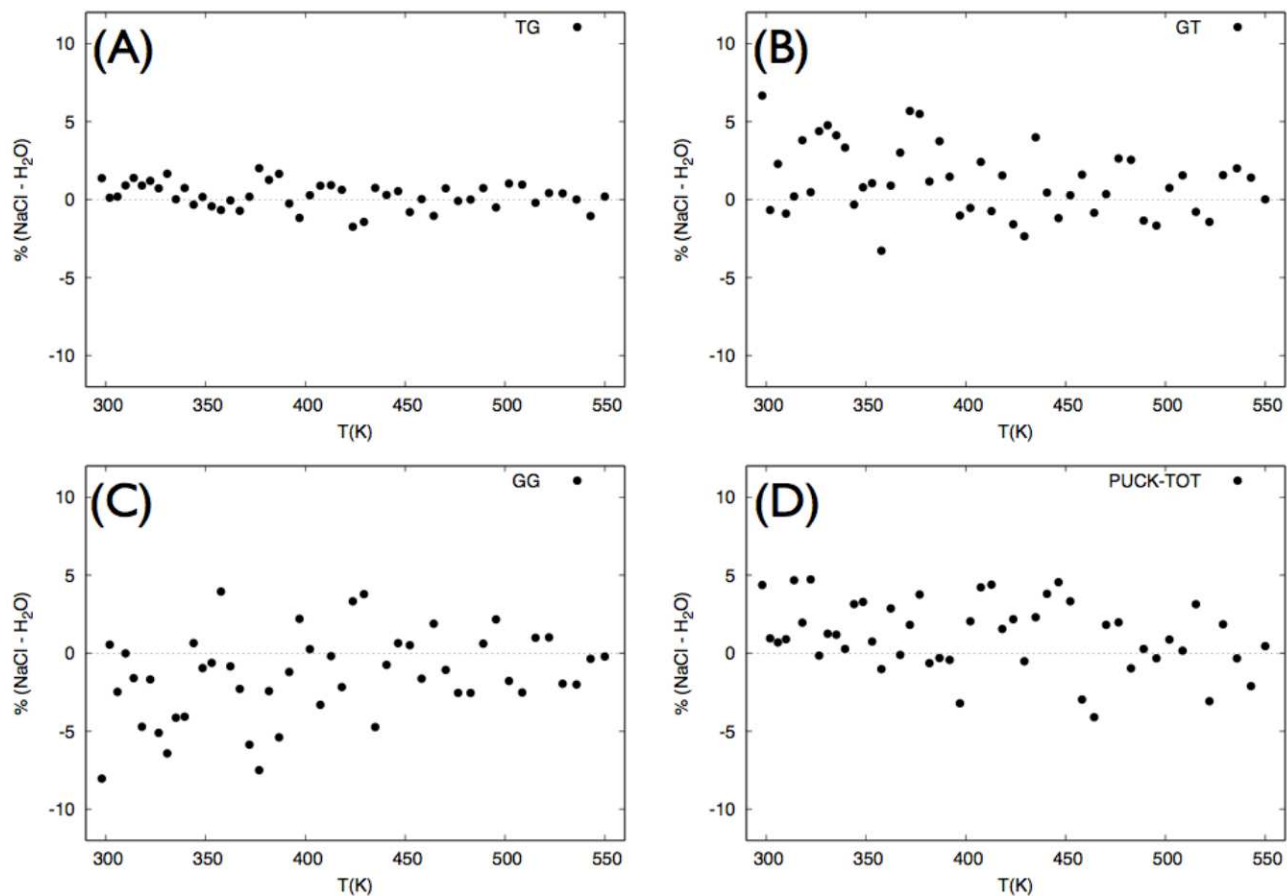


Figure S1: (A), (B) and (C): residuals between cellotretrose *tg*, *gt* and *gg* data, respectively, calculated as the difference between the percentages collected in NaCl aqueous solution (S1(A)) and the analogous data collected from the simulations in pure water. These data show that when NaCl is present, the statistical weight of the *gg* state partially diminishes mostly at the expenses of the *gt* state that becomes moderately more favorable than in pure water. (D): analogous residuals for the statistical weight of the non 4C_1 conformations show a small increment when NaCl is present.

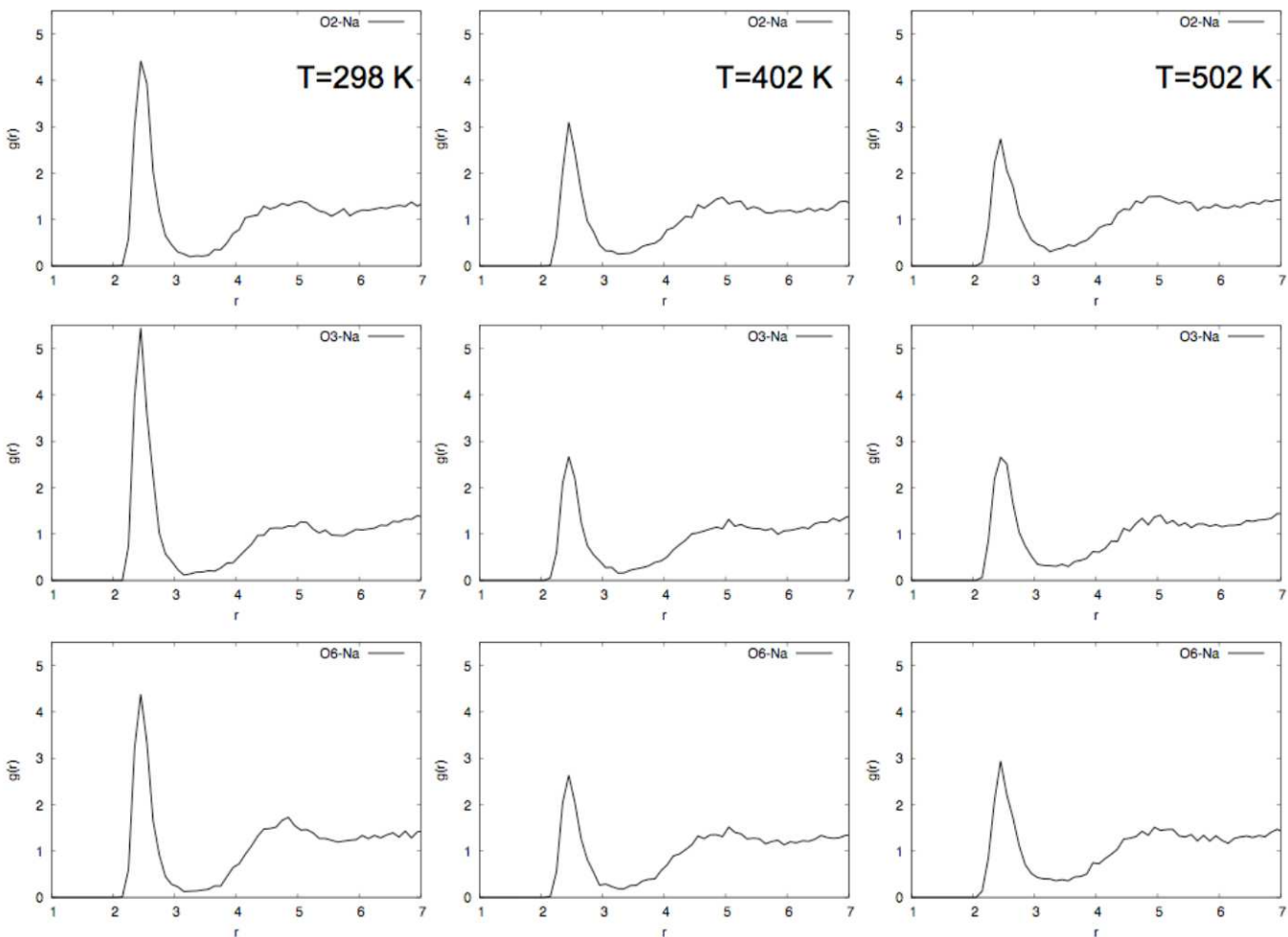


Figure S2: Radial distribution functions for Na^+ and O2 , O3 , and O6 (top, middle, bottom row, respectively) at 298 K, 402 K and 502 K (left, center, right column, respectively).

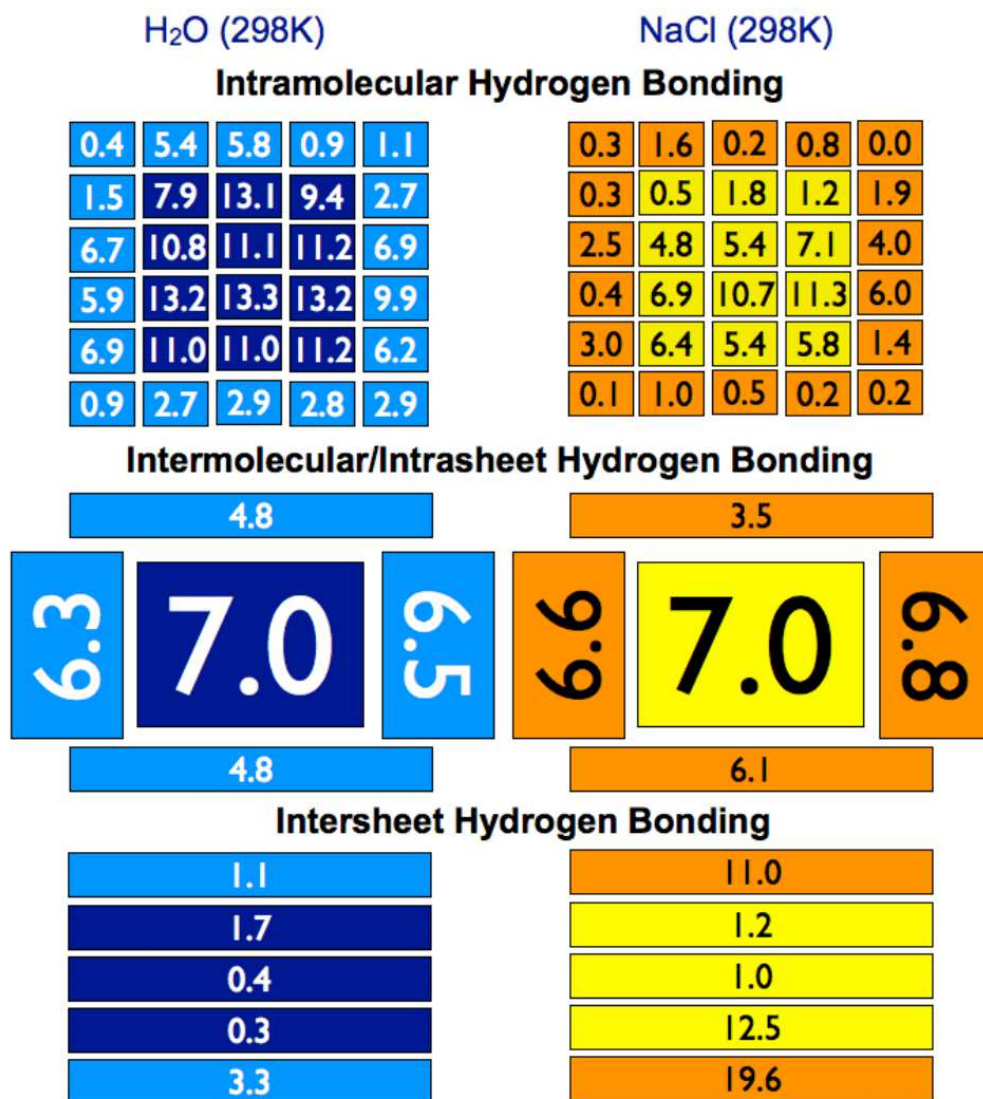


Figure S3: Hydrogen bond network in cellulose I_β in pure water (left) and in NaCl solution (right) at 298 K. The two 6x5 grids on the top row show the average number of intrachain hydrogen bonds per chain. The central row shows the average number of “interchain/intrasheet” hydrogen bonds (between glucan chains within the same fibril’s horizontal layer), while the bottom row shows the average number of “interchain/intersheet” hydrogen bonds (between neighboring layers within the cellulose fibril).

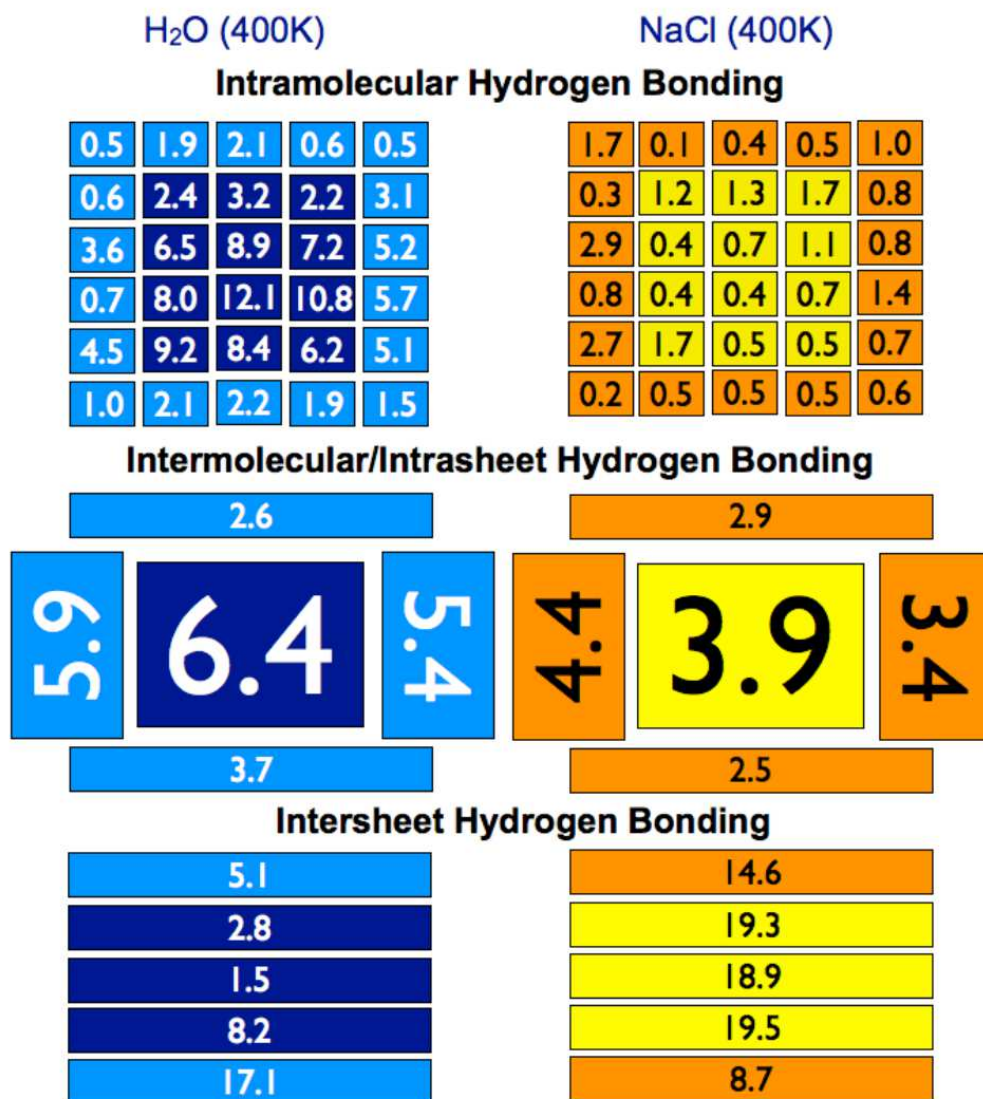


Figure S4: Hydrogen bond network in cellulose I_β in pure water (left) and in NaCl solution (right) at 400 K. The two 6x5 grids on the top row show the average number of intrachain hydrogen bonds per chain. The central row shows the average number of “interchain/intrasheet” hydrogen bonds (between glucan chains within the same fibril’s horizontal layer), while the bottom row shows the average number of “interchain/intersheet” hydrogen bonds (between neighboring layers within the cellulose fibril).